

Interplay between morphology and metallization in amorphous-amorphous transitions

A. Di Cicco,^{1,3,*} A. Congeduti,² F. Coppari,¹ J. C. Chervin,¹ F. Baudelet,² and A. Polian¹

¹IMPMC-CNRS, Université Pierre et Marie Curie, 140 rue de Lourmel, 75015 Paris, France

²Synchrotron Soleil, L'Orme des Merisiers Saint-Aubin, 91192 Gif-sur-Yvette, France

³CNISM, CNR-INFM Soft, Dipartimento di Fisica, Università di Camerino, Via Madonna delle Carceri, I-62032 Camerino (MC), Italy
(Received 13 June 2008; published 30 July 2008)

We present spectacular evidence of metallization of amorphous Ge films under high pressure using optical micrographs and Raman-scattering and x-ray-absorption spectroscopies. This transformation is identified as a low-density amorphous (LDA) to high-density amorphous (HDA) transition, relevant to a large class of systems including amorphous ice, semiconductors, and oxides. We have discovered that this transition initiates at the surface of the LDA sample, characterized intrinsically by a thickness dependent density of voids. Contrary to the case of transitions involving stable crystalline solid phases, our observations show that pressure-induced phase transitions in inhomogeneous amorphous samples are morphology driven and are favored for lower defect (void) densities. The metal disordered phase is observed first at 8 GPa for a lower density of voids, transforming to a metastable ordered phase upon depressurization. The local HDA structure is characterized by an increase in the first-neighbor coordination number, average distance, and variance.

DOI: [10.1103/PhysRevB.78.033309](https://doi.org/10.1103/PhysRevB.78.033309)

PACS number(s): 61.43.Dq, 64.70.-p, 78.30.Ly, 78.70.Dm

The possible occurrence of different structure types for the same disordered substance (polyamorphism) is a fundamental natural effect with strong interdisciplinary implications, ranging from earth and planetary sciences to chemistry and materials science. In recent times, the existence of polyamorphism has been discussed for a variety of systems (see Refs. 1–5 and references therein). Clear evidence for a liquid-liquid transition in a single-component system was obtained for liquid P at high temperatures and pressures.³ Low-density to high-density liquid-liquid phase transitions are likely to occur in liquids with open molecular coordination environments at low pressure such as Si, Ge, C, SiO₂, and GeO₂ and in some metals (see, for example, Ref. 4 and references therein). Analogous transformations are expected to occur in the corresponding glasses, which can be measured in high-pressure experiments.^{6–11} Water is one of the most studied examples of materials for which different glassy polymorphs^{2,5,12} have been experimentally measured.

In simple systems such as amorphous Ge (*a*-Ge) or amorphous Si (*a*-Si) the competition between a low-density amorphous (LDA) and a high-density amorphous (HDA) phase can result in a pressure-induced transition, leading to new properties of these technological materials. However, scattered and conflicting results were obtained in previous works for *a*-Ge. In particular, an onset of metallization and crystallization of thin *a*-Ge films^{13,14} was found at about 6 GPa, while no modifications of the *a*-Ge average structure were observed for pressures below 10 GPa using x-ray-absorption spectroscopy (XAS).^{15,16} Moreover, recent theoretical calculations have indicated that *a*-Si and *a*-Ge undergo transitions to denser structures, although transition pressures differ from those observed experimentally.^{17–19} More recently, evidence for a transition between semiconducting and metallic polymorphs of amorphous silicon was obtained by Raman-scattering and conductance measurements,¹⁰ later studied also by x-ray diffraction.²⁰ The glass transition in Si and Ge was also studied in two recent works,^{9,11} while some of us obtained evidence for the onset of a structural transition in *a*-Ge using x-ray-absorption spectroscopy.⁸

In this work we tackle the problem of a direct *in situ* investigation of the LDA to HDA transition of *a*-Ge under high pressure using optical micrographs and Raman-scattering and x-ray-absorption spectroscopies. The aim is to use the combination of those techniques to shed light on the nature of the LDA-HDA transition accounting for the effect of natural inhomogeneities occurring in controlled preparation conditions in real amorphous samples.

Samples were obtained by evaporation of high-purity Ge, taking care of the possible effects of their morphology and density in the occurrence of the LDA-HDA transition. In fact, amorphous covalent systems, studied in detail in the past due mainly to their technological applications, can show different properties according to the preparation methods. In particular, the macroscopic density of those intrinsically inhomogeneous systems can vary in a quite broad range depending mainly on the density of voids and microscopic defects obtained during growth.^{21,22}

Amorphous Ge films were obtained by evaporation onto a cleaned and degassed glass substrate at ambient temperature and pressure of about 10^{−6} mbar. The rate (about 2 Å/s) and thickness of the deposition were monitored by a calibrated quartz-crystal oscillator. The total thickness was about 3 μm, suitable for x-ray-absorption, diffraction, and optical Raman spectroscopies. The morphology of the films was carefully examined by electron and optical microscopies on the deposited films and on flakes removed from the substrate. Flakes of suitable size have been used as samples for Raman-scattering and x-ray-absorption experiments. As is well known, the LDA short-range structure is practically independent of the preparation method, while the morphology, defects, and density of the samples are sensitive to preparation conditions. In particular, the void fraction is highly thickness dependent²³ and that density tends to an asymptotic limit near to the crystal Ge (*c*-Ge) density for increasing thickness. The micrographs of the surface of our *a*-Ge film (see Fig. 1) show directly this behavior. The surface in direct contact with the substrate (surface S, right picture in the figure) contains a large number of voids with respect to the

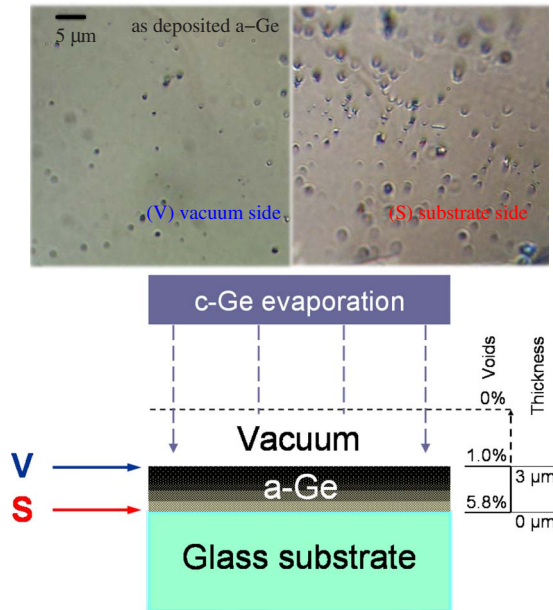


FIG. 1. (Color online) Upper figures: images of the surface of the *a*-Ge film (thickness of about 3 μm) collected using a metallographic optical microscope. The morphologies of the film removed from the evaporation substrate (glass) are different on the two sides. The substrate side S (toward the glass) contains a larger number of voids than the V (vacuum) side. The estimated surface density fraction of voids, evaluated on a set of micrographs, changes from 5.8% to about 1% from the substrate to the vacuum side. Lower figure: section of the sample evaporated on the glass substrate showing the void density change and the S and V sides of the films.

other surface (vacuum surface V, left picture in the figure). Electron microscopy measurements showed that *a*-Ge is otherwise homogeneous down to a scale of about 200 Å and x-ray diffraction showed the characteristic features of LDA *a*-Ge. A section of the *a*-Ge evaporated sample on the glass surface is shown in Fig. 1 (lower panel). The estimated surface density fraction of voids, evaluated on a wide set of micrographs, changes from 5.8% to about 1% from the S to the V side. The inhomogeneous void distribution affects obviously the macroscopic density of the evaporated film. The estimated relative density reduction (with respect to compacted *a*-Ge without voids) is from about 1.4% to 0.1% on approaching the V side, in line with previous estimates of void fraction and density of samples obtained in similar conditions.^{21,23}

The occurrence of a LDA-HDA transition in *a*-Ge has been studied *in situ* by high-pressure Raman and XAS spectroscopies by loading a diamond anvil cell (DAC) with *a*-Ge flakes. The Raman-scattering results are shown in Fig. 2 [panels (a) and (b)] for increasing pressures, along with the micrographs collected at different pressures [panel (c)]. The Raman measurements on *c*-Ge and *a*-Ge samples were performed using a laser wavelength of 540.5 nm (power of up to 750 mW). Best measurements for *a*-Ge were obtained using NaCl as a pressure medium with *a*-Ge flakes in direct contact with the diamond culet. No differences were found in *c*-Ge and *a*-Ge using neon or NaCl pressure mediums in the pressure range under consideration. The Raman pattern shows a

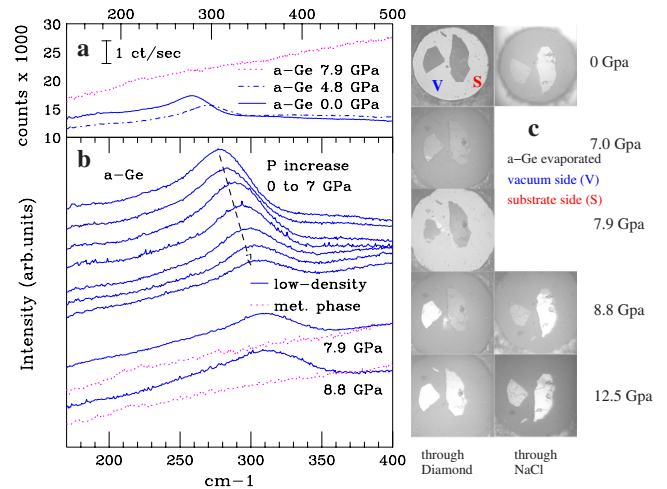


FIG. 2. (Color online) Panel (a): Raman-scattering patterns for HDA (7.9 GPa) and LDA (0 and 4.8 GPa) phases shown on an extended range and on absolute intensity scale. The HDA sample shows a stronger diffuse scattering and loss of Raman signals. Panel (b): *a*-Ge Raman patterns for increasing pressures. The *a*-Ge LDA Raman pattern shows a dominant contribution around 280 cm^{-1} , which shifts to higher frequencies at higher pressures, as a consequence of the bond shortening. The *a*-Ge films undergo a LDA-HDA transition at about 8 GPa which involves the V (vacuum) side of the films. The substrate side (S) is found to be still LDA up to about 10 GPa. Raman measurements at 7.9 and 8.8 GPa are shown for both phases on the two sides of the *a*-Ge films. Panel (c): images of the *a*-Ge sample through the circular gasket hole (initial aperture, 250 μm) for increasing pressure. Two samples have been loaded showing both sides V and S for Raman measurements (through diamond, first column). The rightmost images were collected on the opposite side through the NaCl medium and they show clearly a complementary trend. Most Raman measurements have been performed on the V sample indicated in the figure. The transition to a new phase is clearly visible at 7.9 GPa and is completed at 8.8 GPa. The transition of side S is observed at about 10 GPa (image shown for both sides at 12.5 GPa).

dominant contribution by the tetrahedral stretching vibrations around 280 cm^{-1} . The *a*-Ge Raman features reflect the broadening of the *c*-Ge phonon density of states, containing transverse-optical (TO) modes (300 cm^{-1}) as well as weaker features associated with longitudinal-optical (LO) and acoustic modes (around 220 and 80 cm^{-1} , respectively; see the calculations in Ref. 24). As shown in Fig. 2(b), the bands shift to higher frequencies at higher pressures, as a consequence of the bond shortening. We observe a clear transition at about 8 GPa which involves the surface of the V side of the films. The transition of the substrate side S is shifted to about 10 GPa (last measurement of a LDA Raman pattern). This is shown also by the micrographs obtained through the gasket hole for increasing pressure, reported in Fig. 2(c). Two film samples have been loaded showing both sides (V and S) for Raman measurements [through diamond, first column of Fig. 2(c)]. The transition to a new phase is clearly visible at 7.9 GPa and is completed at 8.8 GPa. The new high-pressure phase shows a metal-like reflectivity, stronger diffuse scattering, and loss of Raman signals, compatible with a metallic character. Upon releasing the pressure, the

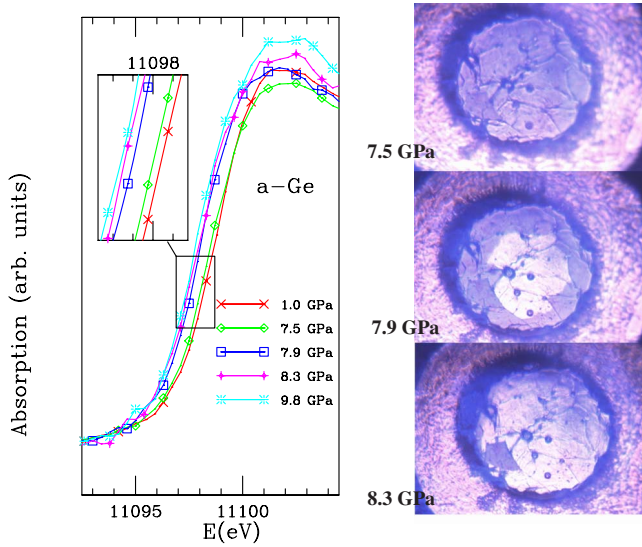


FIG. 3. (Color online) Left panel: shift of the Ge K edge structure at high pressures (all data normalized to 1). The shift to lower energies around 8 GPa is associated with the disappearance of the gap in a metallic state. Right panel: micrographs of the a -Ge sample through the diamonds. The transition to a highly reflective metallic state is clearly visible.

metallic HDA phase transforms to a metastable solid crystalline phase (called GeIII or ST12; see Refs. 25 and 26 and references therein), as shown by a typical Raman-scattering pattern. The GeIII local structure is known to be tetrahedral-like, although much denser than the stable diamond phase. Transition to the GeIII phase was not observed on the S side of the sample upon releasing the pressure. The samples, returned to ambient pressure after several pressure cycles, were observed to transform again to a disordered LDA phase at pressures below 1 GPa. Full details of the observations upon depressurization will be given elsewhere.

A proof of the metallic character of the new phase has been obtained by looking at the shift of the Ge K edge position at high pressure, shown in Fig. 3 (left panel). The spectra reported in Fig. 3 were obtained by loading a DAC with two superimposed LDA a -Ge flakes filling completely the gasket hole (micrographs in Fig. 3, right) in order to have a homogeneous thickness of about 6 μm . The DAC has been positioned on the new XAS dispersive beamline ODE at Soleil synchrotron radiation facility. Several XAS measurements of up to about 10 GPa were performed, showing the clear edge shift of about 1 eV associated with the closure of the gap at 7.9 GPa.²⁷ The metallization has been clearly observed also in the optical micrographs shown in Fig. 3 (right panel).

A deeper insight on the nature of the phase transition has been achieved by collecting and analyzing XAS data in an extended range as shown in Fig. 4. The trend of the measured XAS $k\chi(k)$ as a function of increasing pressure is shown in Fig. 4, panel (a). The occurrence of the transition is clearly visible between 7.9 and 8.3 GPa, where the intensity of the signal dramatically decreases and the oscillation frequency increases. The Fourier transform (FT) is shown in panel (b) and the sudden intensity change can be appreciated

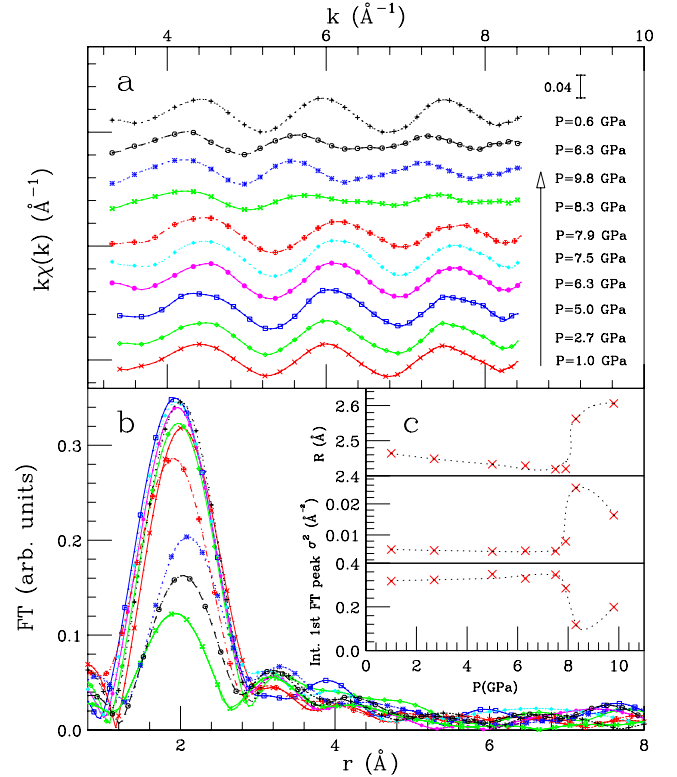


FIG. 4. (Color online) Panel (a): measured XAS $k\chi(k)$ data during a compression-decompression cycle shown from the bottom to the top. The data were smoothed for clarity of the presentation. The dramatic intensity and phase change of the signal associated with the LDA-HDA transition is clearly visible in the data above 7.9 GPa. Panel (b): the FT of the experimental data shows a clear trend of the intensity (shown in the inset) and position of the first peak. Inset (c): average first-neighbor distance R and variance σ^2 obtained by XAS data analysis shown as a function of pressure. The structural changes associated with the transition are clearly visible looking at the sudden increases in R and σ^2 (intensity decrease of the first FT peak).

looking at the trend of the first FT peak intensity shown in inset (c). The drop in intensity occurring around 8 GPa is followed by an increase around 10 GPa. The XAS signals were analyzed by GNXAS (Ref. 27) using a simple first-neighbor model distribution which has been already shown to be effective in previous studies.²⁷ The average distances and the variances of the first neighbors are plotted in inset (c) of Fig. 4 as a function of pressure. The average distance R shows a monotonic shortening up to 7.9 GPa, at which an abrupt elongation is found. At the same time, the structural disorder associated with the bond-length variance σ^2 is found to increase at 7.9 GPa, reaching in the HDA structure values that are five times higher than those related to the LDA phase. The first-neighbor coordination number (CN) is found to increase substantially above 8 GPa from the initial LDA value (4), reaching the typical values of a metallic β -tin structure (5 ± 1 at 8.3 GPa and 6 ± 0.5 at 9.8 GPa). The increase in the first-neighbor CN and of the bond-length variances and distances are consistent with the transition to a HDA phase above 8 GPa.

In conclusion, our experimental results demonstrate that the LDA-HDA transition in evaporated *a*-Ge films involves a metallization beginning on the uppermost layers at about 8 GPa. The transition is revealed directly by optical micrographs, Raman spectroscopy, and XAS. The HDA phase has been found to crystallize in a dense metastable crystalline phase upon decreasing the pressure, which then becomes LDA again at ambient pressure. Contrary to the case of the phase changes involving stable crystalline systems (melting and solidification), our direct observation of the LDA-HDA

transition in metastable *a*-Ge shows that the void density and morphology of the specimen are important factors affecting the onset of the transition. The fact that such a pressure-induced phase transition is favored for lower defect densities can have different explanations related to both the inhomogeneous density change under pressure and the presence of surface stresses affecting the pressure field inside the sample. The results of this work will thus stimulate further experimental and theoretical studies for understanding phase transition in intrinsically inhomogeneous disordered systems.

*Permanent address: CNISM, CNR-INFM Soft, Dipartimento di Fisica, Università di Camerino, Via Madonna delle Carceri, I-62032 Camerino (MC), Italy.

- ¹P. H. Poole, T. Grande, C. A. Angell, and P. F. McMillan, *Science* **275**, 322 (1997).
- ²O. Mishima and H. E. Stanley, *Nature (London)* **396**, 329 (1998).
- ³Y. Katayama, T. Mizutani, W. Utsumi, O. Shimomura, M. Yamakata, and K. Funakoshi, *Nature (London)* **403**, 170 (2000).
- ⁴G. Franzese, G. Malescio, A. Skibinsky, S. V. Buldyrev, and H. E. Stanley, *Nature (London)* **409**, 692 (2001).
- ⁵O. Mishima and Y. Suzuki, *Nature (London)* **419**, 599 (2002).
- ⁶M. Grimsditch, *Phys. Rev. Lett.* **52**, 2379 (1984).
- ⁷J. P. Itié, A. Polian, G. Calas, J. Petiau, A. Fontaine, and H. Tolentino, *Phys. Rev. Lett.* **63**, 398 (1989).
- ⁸E. Principi, A. Di Cicco, F. Decremps, A. Polian, S. De Panfilis, and A. Filipponi, *Phys. Rev. B* **69**, 201201(R) (2004).
- ⁹A. Hedler, S. L. Klaumunzer, and W. Wesch, *Nat. Mater.* **3**, 804 (2004).
- ¹⁰P. F. McMillan, M. Wilson, D. Daisenberger, and D. Machon, *Nat. Mater.* **4**, 680 (2005).
- ¹¹M. H. Bhat, V. Molinero, E. Soignard, V. C. Solomon, S. Sastry, J. L. Yarger, and C. A. Angell, *Nature (London)* **448**, 787 (2007).
- ¹²P. G. Debenedetti and F. H. Stillinger, *Nature (London)* **410**, 259 (2001).
- ¹³O. Shimomura, S. Minomura, N. Sakai, K. Asaumi, K. Tamura, J. Fukushima, and H. Endo, *Philos. Mag.* **29**, 547 (1974).
- ¹⁴K. Tanaka, *Phys. Rev. B* **43**, 4302 (1991).
- ¹⁵J. Freund, R. Ingalls, and E. D. Crozier, *J. Phys. Chem.* **94**, 1087 (1990).
- ¹⁶J. P. Itié, A. Polian, D. Martinez-Garcia, V. Briois, A. Di Cicco, A. Filipponi, and A. San Miguel, *J. Phys. IV* **7**, C2 (1997).
- ¹⁷M. Durandurdu and D. A. Drabold, *Phys. Rev. B* **66**, 041201(R) (2002).
- ¹⁸M. Durandurdu and D. A. Drabold, *Phys. Rev. B* **67**, 212101 (2003).
- ¹⁹J. Koga, K. Nishio, T. Yamaguchi, and F. Yonezawa, *J. Phys. Soc. Jpn.* **73**, 388 (2004).
- ²⁰D. Daisenberger, M. Wilson, P. F. McMillan, R. Quesada Cabrera, M. C. Wilding, and D. Machon, *Phys. Rev. B* **75**, 224118 (2007).
- ²¹D. K. Pandya, A. C. Rastogi, and K. L. Chopra, *J. Appl. Phys.* **46**, 2966 (1975).
- ²²T. M. Donovan and K. Heinemann, *Phys. Rev. Lett.* **27**, 1794 (1971).
- ²³P. J. McMarr, J. R. Blanco, K. Vedam, R. Messier, and L. Pili-ione, *Appl. Phys. Lett.* **49**, 328 (1986).
- ²⁴R. Alben, D. Weaire, J. E. Smith, and M. H. Brodsky, *Phys. Rev. B* **11**, 2271 (1975).
- ²⁵A. Di Cicco, A. C. Frasini, M. Minicucci, E. Principi, J. P. Itié, and P. Munsch, *Phys. Status Solidi B* **240**, 19 (2003).
- ²⁶C. S. Menoni, J. Z. Hu, and I. L. Spain, *Phys. Rev. B* **34**, 362 (1986).
- ²⁷A. Filipponi and A. Di Cicco, *Phys. Rev. B* **51**, 12322 (1995).